The E166 Experiment: Undulator Based Production of Polarized Positrons

Hermann Kolanoski (for the E166 Collaboration)

Humboldt-Universität zu Berlin

Abstract. The E166 experiment at the Stanford Linear Accelerator Center (SLAC) has demonstrated a scheme for the production of polarized positrons which is suitable for implementation in a future Linear Collider. A multi-GeV electron beam passed through a helical undulator to generate multi-MeV, circularly polarized photons which were then converted in a thin target to produce positrons (and electrons) with longitudinal polarization above 80% at 6 MeV. The results are in agreement with GEANT4 simulations that include the dominant polarization-dependent interactions of electrons, positrons and photons in matter.

Keywords: helical undulator, positron, polarization
PACS: 07.77.Ka, 13.88.+e, 29.27.Hj, 41.75.Fr

1. INTRODUCTION

The conceptual design of a future electron-positron linear collider, the International Linear Collider (ILC), is currently pursued through an international effort [1]. Scientifically, the ILC experiments will cover the energy range where the Higgs boson, Supersymmetry and other 'physics beyond the Standard Model' are expected. The ILC capabilities of identifying new particles by determining their quantum numbers and the Lorentz structure of their couplings are largely enhanced if the electron and positron beams are both polarized [2]. While the generation of polarized electrons is standard procedure, polarized positron sources with sufficient intensity are not existing. However, even in those cases where in principle the polarization of only one beam is sufficient, the polarization of both beams has large advantages: the higher effective polarization allows a better background reduction and at the same time a selective enhancement of the channel of interest, thereby providing clearer signatures and improved statistical accuracy. There are also cases which are only measurable if both beams are polarized, an example of this would be the separation of the selectrons which are partners to either the left-handed or right-handed electrons/positrons [2].

Polarized positrons can be generated via the pair production process by circularly polarized photons [3]. Different methods have been proposed to generate polarized photons. In the scheme proposed by Balakin and Mikhailichenko [4] the photons are produced by passing a multi-GeV electron beam through a helical undulator producing multi-MeV photons with circular polarization [5]. Alternatively, circularly polarized photons can also be produced by backscattering circularly polarized laser photons off an electron beam [6].

The E166 experiment [7, 8], described in this paper, has demonstrated that a polarized positron source based on the helical undulator scheme is suited for use at the ILC.

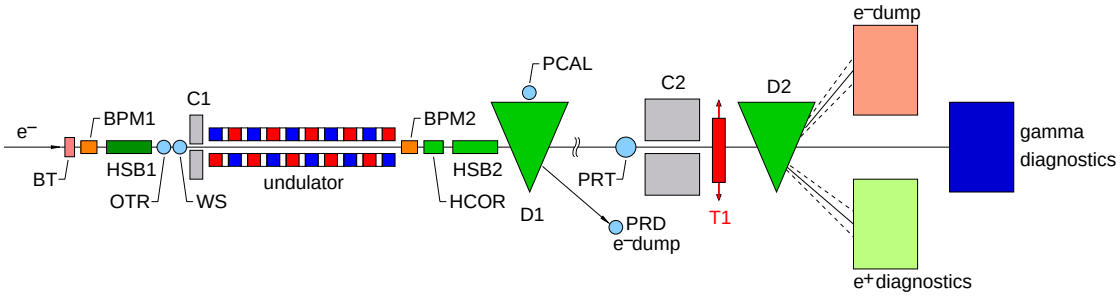

FIGURE 1. Conceptual layout (not to scale) of the E166 experiment in the SLAC FFTB. The electrons enter from the left and, after traversing the undulator, are dumped using magnet D1. The positron production target T1 and the positron and photon diagnostics are located 35 m downstream of the undulator. The spectrometer D2 allows to measure the energy dependence of the positron polarization. The labels BPM, HSB, OTR, BT, WS, HCOR, PCA, PRD, PRT indicate beam monitoring and steering devices and C1, C2 are aperture limiting collimators.

2. EXPERIMENTAL SETUP

The E166 experiment was carried out at the Final Focus Test Beam (FFTB) facility [9] at SLAC. Figure 1 shows a schematic layout of the experiment. A 46.6 GeV electron beam from the linac was passed through a 1 meter long pulsed helical undulator to generate polarized photons, the photon beam was then converted in a thin target to electron-positron pairs and the photons and positrons were analyzed for their polarization.

Undulator. A helical undulator consists of two wires wound adjacent to each other helically around a tube (Fig. 2 left). Electrical currents are sent in opposite directions through the wires thereby creating a magnetic field spiraling along the longitudinal helix axis. An electron beam propagating on axis through the undulator radiates circularly polarized photons due to interaction with the spiraling field. Parameters describing the behavior of an undulator are the energy of the electron beam, the helical period of the undulator and the so-called K-parameter which determines the photon intensity and spectrum (Fig. 2 right).

The E166 undulator was operated at a pulsed current of 2.3 kA, a pulse duration of about 12 μs and a repetition rate of 10 Hz. The positioning and alignment of the high-energy electron beam through the nominal 0.87 mm diameter aperture of the 1 meter long undulator presented special challenges.

Positron generation, transport and diagnostics. The undulator photons impinged on the conversion target T1 (0.2 r.l. tungsten) to produce electron-positron pairs (Fig. 1). Figure 3 depicts the diagnostics for photons and positrons beyond T1.

Photon polarimetry. The polarization of the MeV-photons from the undulator was determined using Compton transmission polarimetry which exploits the spin dependence of photon transmission through magnetized iron. The transmission asymmetry for opposite magnetizations, $\delta = (T^+ - T^-)(T^+ + T^-) \sim P_\gamma$, was measured behind the analyzer magnet TP2 (Fig. 3) using different detectors.

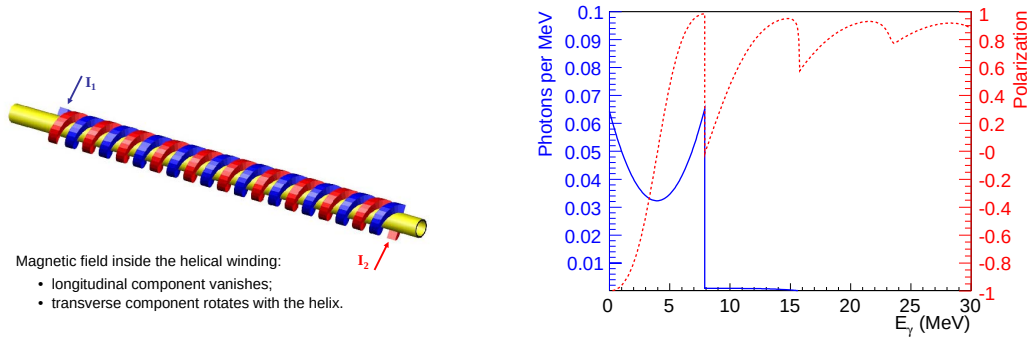

FIGURE 2. Left: Sketch of the left-handed, bifilar windings of the undulator. Right: The solid line shows the calculated photon number spectrum per beam electron of undulator radiation integrated over angle, plotted as a function of photon energy E_γ for electron beam energy 46.6 GeV, undulator period 2.54 mm and undulator strength parameter $K = 0.17$. The peak energy of the first harmonic (dipole) radiation was 7.9 MeV. The dashed line shows the longitudinal polarization P_γ of the undulator radiation as a function of energy.

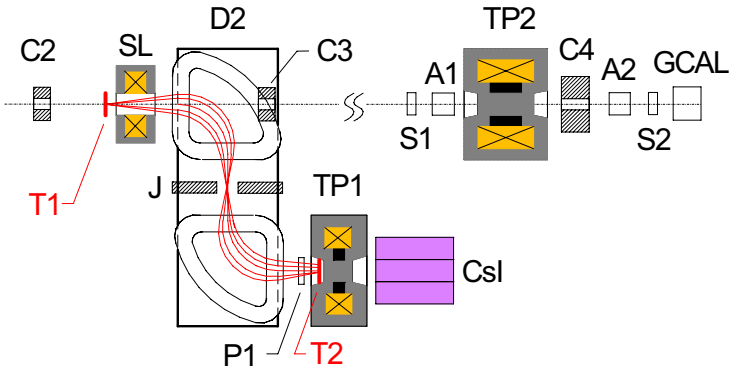

FIGURE 3. Schematic of the photon and positron diagnostics. SL = solenoid lens; D2 = dipole spectrometer magnet; J = movable jaws; C2-C4 = collimators; T1 = positron production target; T2 = reconversion target; TP1 = positron transmission polarimeter solenoid; TP2 = photon transmission polarimeter solenoid; CsI = 3×3 array of CsI crystals; GCAL = Si-W calorimeter; A1, A2 = aerogel Cherenkov detectors; P1, S1, S2 = Si-diode detectors.

Positron polarimetry. Compton transmission polarimetry was also employed to determine the positron polarization. This was possible by first transferring the positron polarization to photons via Bremsstrahlung and annihilation processes in a "reconversion" target (T2 in Fig. 3).

After generating polarized positrons in the conversion target (T1) the positrons passed through the spectrometer (SL+D2) which selected energy and focused the positrons onto the 'reconversion' target T2 (0.5 r.l. tungsten). The number of positrons intercepted by the target was counted in the silicon counter P1. The photons generated in the reconversion target partly inherited the positron polarization. The energy of the photons which traversed the magnetized iron core of the analyzer magnet TP1 was measured in the CsI calorimeter behind the magnet. The asymmetry δ of the energy deposition

for opposite magnetization directions is related to the analyzing power A, the electron polarization in the iron, P^{Fe}, and the positron polarization P_{e^+} by

$$A = \frac{\delta}{P^{\mathrm{Fe}} P_{e^+}}. \tag{1}$$

The analyzing power was determined for different energy settings employing detailed simulations of polarization dependent cross sections in the reconversion target and the analyzer magnet. The simulation package GEANT4 has been extended to include spin dependence of the dominant electromagnetic processes [10].

3. DATA ANALYSIS AND RESULTS

Photon asymmetries. For the undulator photons the transmission asymmetries were measured behind the analyzer magnet TP2 with the three different detectors shown in Fig. 3. Since the transmission was obtained for the full undulator spectrum it was not possible to derive a polarization value for specific photon energies. Thus the measured asymmetries have just been compared to predictions from detailed simulations (the detectors have different energy thresholds and spectral sensitivities):

detector	asymmetry δ (%)	predicted δ (%)
S2 (silicon)	$3.88 \pm 0.12 \pm 0.63$	3.1
A2 (aerogel)	$3.31 \pm 0.06 \pm 0.16$	3.6
GCAL (Si/W)	$3.67 \pm 0.07 \pm 0.40$	3.4

Reasonable agreement with expectations was found for all detectors thus confirming the expected functionality of the undulator.

Positron asymmetries. A relatively large background, which was not associated with undulator photons, had to be taken into account to determine the positron induced energy deposition in the CsI calorimeter. This was done by pulsing the undulator only every other linac pulse (technically the undulator current pulse was just shifted in time). Figure 4 shows the distribution of undulator-on and undulator-off energy depositions in the central CsI crystal.

The data were taken in 'cycles' with the polarity of the analyzer magnet reversed for every other cycle. A cycle contained about 3000 events, alternating between undulator-on and undulator-off. For each cycle the corrected mean energy deposition was determined by plotting for all possible 'on-off' combinations (ij) the differences:

$$E_{ij} = E_{ij}^{\mathrm{on}} - E_{ij}^{\mathrm{off}} = \frac{E_i^{\mathrm{on}} - E_j^{\mathrm{off}} \frac{I_i^{\mathrm{on}}}{I_j^{\mathrm{off}}}}{\mathsf{P1}_i^{\mathrm{on}} - \mathsf{P1}_j^{\mathrm{off}} \frac{I_i^{\mathrm{on}}}{I_j^{\mathrm{off}}}}. \tag{2}$$

That means, the measured energy depositions were corrected for the actual currents $I_{i,j}^{\mathrm{on,off}}$ in each event and normalized to the number of positrons measured in the counter

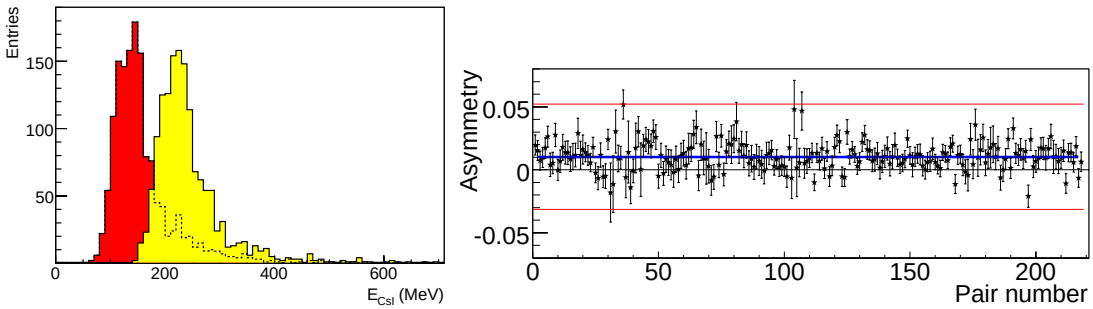

FIGURE 4. Left: Examples of energy distributions for events in the central CsI crystal (red/dark: undulator off, yellow/light: undulator on). Right: Positron-induced asymmetries δ_{e^+} in the central CsI crystal of the positron polarimeter for 220 pairs of cycles with opposite magnetization in the polarimeter. The central positron energy was 6.1 MeV. The average asymmetry was 0.0113, as indicated by the horizontal line.

TABLE 1. Positron (electron) asymmetries, analyzing powers and polarizations for different energies.

$E_{e^\pm}$ [MeV]	$\delta \pm \sigma_\delta$(stat) [%]	A	$P \pm \sigma_P$(stat) $\pm \sigma_P$(sys) [%]
4.6 (e^+)	0.69 ± 0.17	0.150	$66 \pm 16 \pm 8$
5.4 (e^+)	0.96 ± 0.08	0.156	$89 \pm 8 \pm 9$
6.1 (e^+)	1.13 ± 0.06	0.162	$96 \pm 6 \pm 10$
6.7 (e^+)	0.92 ± 0.08	0.165	$80 \pm 7 \pm 9$
6.7 (e^-)	0.94 ± 0.05	0.153	$88 \pm 5 \pm 15$
7.4 (e^+)	0.89 ± 0.20	0.169	$76 \pm 17 \pm 12$

P1 in front of the reconversion target (Fig. 3). The distribution of the E_{ij} (for each cycle) was fitted with two Gaussian functions (to account for the non-Gaussian tails). The average corrected signal energy S_{CsI} has been determined from the mean of all entries in the distribution within $\pm 2\sigma$ of the narrower Gaussian. This 'truncated mean' of all on-off combinations was found to be most efficient in eliminating the non-Gaussian fluctuations.

Using the corrected mean energy depositions the asymmetries were determined for each cycle pair with opposite magnetization (associating pairs in chronological order): $\delta = (S^-_{\mathrm{CsI}} - S^+_{\mathrm{CsI}})(S^-_{\mathrm{CsI}} + S^+_{\mathrm{CsI}})$. The asymmetries are plotted in Fig. 4 (right) for all analyzed cycle pairs of a particular spectrometer setting. The average asymmetries for each spectrometer setting are recorded in Table 1.

Positron polarization. Inverting the formula for the analyzing power (1) the positron polarization was determined from

$$P_{e^+} = \frac{\delta}{A\,P^{\mathrm{Fe}}}. \tag{3}$$

The results for different energies are shown in Fig. 5 and are recorded together with the asymmetries and analyzing powers in Table 1. In addition to five positron energy points the electron polarization was measured for one energy as a check of systematic uncertainties (the stray field of the analyzer magnet affects electrons and positrons differently). The measurements are compared in Fig. 5 with the expectations obtained

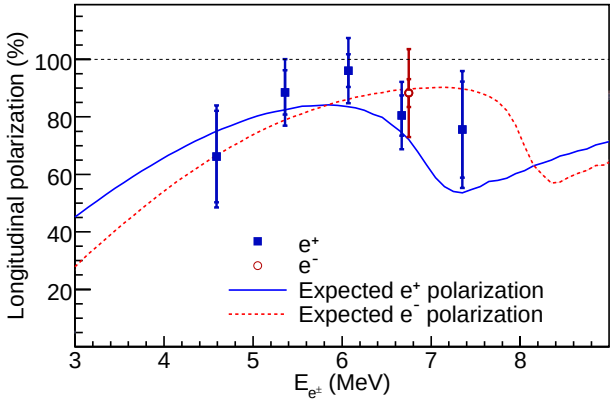

FIGURE 5. Longitudinal polarization $P_{e^\pm}$ as a function of energy $E_{e^\pm}$ of positrons and electrons as determined from the asymmetries observed in the central CsI crystal. The smaller error bars show the statistical uncertainty, and the larger bars indicate the statistical and systematic uncertainties combined in quadrature. Also shown are predictions by a GEANT4 simulation of the experiment.

from simulations. Within the given statistical and systematic uncertainties the agreement is very good.

4. SUMMARY

The E166 experiment has been carried out in the Final Focus Test Beam at SLAC to demonstrate production of polarized positrons suitable for implementation at the ILC. A 1 meter long helical undulator of 2.54 mm period produced circularly polarized photons (1st harmonic endpoint 7.9 MeV for a 46.6 GeV beam). The polarized photons were converted to polarized positrons in a thin target and analyzed by transmission polarimetry of photons obtained on "reconversion" of the positrons. The measured polarization reached 80% for positrons near 6 MeV and 90% for electrons near 7 MeV. The measurements agree well with simulations made with an upgraded GEANT4 version including the dominant polarization-dependent electromagnetic interactions.

REFERENCES

1. *International Linear Collider Reference Design Report* (Aug. 2007), http://www.linearcollider.org/rdr
2. G. A. Moortgat-Pick et al., Phys. Rept. **460**, 131 (2008).
3. H. Olsen and L.C. Maximon, Phys. Rev. **114**, 887 (1959).
4. V.E. Balakin and A.A. Mikhailichenko, Budker Institute of Nuclear Physics, BINP 79-85 (1979).
5. R.C. Wingerson, Phys. Rev. Lett. **6**, 446 (1961).
6. E.G. Bessonov and A.A. Mikhailichenko, Budker Institute of Nuclear Physics, BINP 92-43 (1992); T. Omori et al., Phys. Rev. Lett. **96**, 114801 (2006).
7. G. Alexander et al., Phys. Rev. Lett. **100**, 210801 (2008).
8. G. Alexander et al., to be submitted to Nucl. Instr. and Meth. A.
9. M. Berndt et al., SLAC-376 (Mar. 1991).
10. R. Dollan, K. Laihem and A. Schälicke, Nucl. Instr. and Meth. A **559**, 185 (2006); A. Schälicke, K. Laihem and P. Starovoitov, DESY 07-202 (Nov. 2007).